

# Linearized Morison Drag for Improvement Semi-Submersible Heave Response Prediction by Diffraction Potential

Siow, C. L.<sup>a</sup>, Jaswar Koto,<sup>a, b,\*</sup> Hassan Abyn,<sup>a</sup> and N.M Khairuddin,<sup>a</sup>

<sup>a)</sup> Aeronautical, Automotive and Ocean Engineering, Universiti Teknologi Malaysia, Malaysia

<sup>b)</sup> Ocean and Aerospace Research Institute, Indonesia

\*Corresponding author: jaswar.koto@gmail.com

## Paper History

Received: 20-March-2014

Received in revised form: 3-April-2014

Accepted: 10-April-2014

## ABSTRACT

This research is targeted to improve the semi-submersible heave response prediction by using diffraction potential theory by involving drag effect in the calculation. The comparison to the experimental result was observed that heave motion tendency predicted by the diffraction potential theory is no agreed with motion experimental result when the heave motion is dominated by damping. In this research, the viscous damping and drag force for heave motion is calculated from the drag term of Morison equation. The nonlinear drag term in Morison equation is linearized by Fourier series linearization method and then inserted into the motion equation to correct the inadequate of diffraction potential theory. The proposed numerical method is also applied to simulate the semi-submersible motion response to obtain the heave motion tendency predicted by this numerical method. In comparison to the experimental result which tested at the same wave condition obtained that the diffraction potential theory with the Morison drag term correcting is able to provide satisfying heave response result especially in damping dominated region.

**KEY WORDS:** *Morison Equation, Diffraction Potential Theory, Semi-submersible, Motion Response, Viscous Damping.*

## 1.0 INTRODUCTION

This work is targeted to propose a correction method which applicable to linear diffraction theory in order to evaluate the

motion response of selected offshore floating structure. The linear diffraction theory estimate the wave force on the floating body based on frequency domain and this method can be considered as an efficient method to study the motion of the large size floating structure with acceptable accuracy. The effectiveness of this diffraction theory apply on large structure is due to the significant diffraction effect exist on the large size structure in wave [17]. However, some offshore structure such as semi-submersible, TLP and spar are looked like a combination of several slender bodies as an example, branching for semi-submersible.

In this study, semi-submersible structure is selected as an offshore structure model since this structure is one of the favours structure used in deep water oil and gas exploration area. To achieve this objective, a programming code was developed based on diffraction potential theory and it is written in visual basic programming language. By comparing the numerical result predicted by using diffraction potential theory to experiment result, it is obtained that the motion prediction by diffraction potential theory has an acceptable accuracy mostly, except for heave motion when the wave frequency near to the structure natural frequency [18, 19].

As presented in a previous paper, the diffraction potential theory is less accurate to predict the structure heave motion response when the wave frequency closer to structure natural frequency. At this situation, the heave response calculated by the diffraction potential theory will be overshooting compare to experiment result due to low damping executed by the theory and then follow by the large drop which give and underestimating result compare to experiment result before it is returned into normal tendency [18].

In order to correct the over-predicting phenomenon made by the diffraction potential theory, the previous research was trying to increase the damping coefficient by adding viscous damping into the motion equation [19]. From that study, the viscous damping is treated as extra matrix and added into the motion equation separately. This addition viscous damping was estimated based on the equation provided by S. Nallayarasu and P. Siva Prasad in their published paper [20].

By adding the extra viscous damping into the motion equation, it can be obtained that the significant over-predicting of heave motion when wave frequency near to the floating structure natural frequency was corrected and it is close to the experimental result compared to executed result by diffraction potential theory alone [19]. However, the under-predicting of the heave response by diffraction potential theory in a certain wave frequency region still remaining unsolved by adding the viscous damping to the motion equation as discussed in the previous study [19].

In this paper, the discussion will focus on the effect drag force and viscous damping in estimate the semi-submersible heave response using diffraction potential theory. To able the numerical solution to calculate the extra drag force and viscous damping, the drag term in Morison equation is applied here. Accuracy of this modification solution also checked with the previous semi-submersible experiment result which carried out at the towing tank belongs to Universiti Teknologi Malaysia [12, 18]. The experiment is conducted in head sea condition and slack mooring condition for wavelength around 1 meter to 9 meters. In the comparison, it is obtained that the non-agreed heave response tendency near the structure natural frequency predicted by diffraction potential theory can be corrected by involving the drag effect in the calculation.

## 2.0 LITERATURE REVIEW

Hess and Smith, Van Oortmerssen and Loken studied on non-lifting potential flow calculation about arbitrary 3D objects [1, 2, 3]. They utilized a source density distribution on the surface of the structure and solved for distribution necessary to lake the normal component of fluid velocity zero on the boundary. Plane quadrilateral source elements were used to approximate the structure surface, and the integral equation for the source density is replaced by a set of linear algebraic equations for the values of the source density on the quadrilateral elements. By solving this set of equations, the flow velocity both on and off the surface was calculated. Besides, Wu et al. also studied on the motion of a moored semi-submersible in regular waves and wave induced internal forces numerically and experimentally [4]. In their mathematical formulation, the moored semi-submersible was modelled as an externally constrained floating body in waves, and derived the linearized equation of motion.

Yilmaz and Incecikanalyzed the excessive motion of moored semi-submersible [5]. They developed and employed two different time domain techniques due to mooring stiffness, viscous drag forces and damping. In the first technique, first-order wave forces acting on structure which considered as a solitary excitation forces and evaluated according Morison equation. In second technique, they used mean drift forces to calculate slowly varying wave forces and simulate for slow varying and steady motions. Söylemez developed a technique to predict damaged semi-submersible motion under wind, current and wave [6]. He used Newton's second law for approaching equation of motion and developed numerical technique of nonlinear equations for intact and damaged condition in time domain.

Clauss et al. analyzed the sea-keeping behavior of a semi-submersible in rough waves in the North Sea numerically and experimentally [7]. They used panel method TiMIT (Time-domain investigations, developed at the Massachusetts Institute of

Technology) for wave/structure interactions in time domain. The theory behind TiMIT is strictly linear and thus applicable for moderate sea condition only.

An important requirement for a unit with drilling capabilities is the low level of motions in the vertical plane motions induced by heave, roll and pitch. Matos et al. were investigated second-order resonant of a deep-draft semi-submersible heave, roll and pitch motions numerically and experimentally [8]. One of the manners to improve the hydrodynamic behavior of a semi-submersible is to increase the draft. The low frequency forces computation has been performed in the frequency domain by WAMIT a commercial Boundary Element Method (BEM) code. They generated different number of mesh on the structure and calculated pitch forces.

Due to the complexity of actual structures' hull form, S. Nallayarasu and P. Siva Prasad were used experimental and numerical software (ANSYS AQWA) to study the hydrodynamic response of an offshore spar structure which linked to semi-submersible under regular waves. From both the experimental and numerical result, it is obtained that the response of the spar is reduced after linked to semi-submersible due to the interaction of radiation wave generated by both the structures and the motion of spar may be reduced by semi-submersible. However, the research also obtained that the motion response for unmoored semi-submersible is increased when linked to spar [20].

Wackers et al. was reviewed the surface discretisation methods for CFD application with different code [9]. Besides, simulation of fluid flow Characteristic around Rounded-Shape FPSO was also conducted by A. Efi et al. using RANs Method [10]. Jaswar et al. were also developed integrated CFD simulation software to analyze hull performance of VLCC tanker. The integrated CFD simulation tool was developed based on potential theory and able to simulate wave profile, wave resistance and pressure distribution around ship hull [11].

In addition, few experiment tests were carried out to obtain the motion response of semi-submersible. A model test related to interaction between semi-submersible and TLP was carried out by Hassan Abyn et al. [12]. In continue Hassan Abyn et al. also tried to simulate the motion of semi-submersible by using HydroSTAR and then analyse the effect of meshing number to the accuracy of execution result and execution time [13]. Besides, C. L. Siow et al. also make a comparison on the motion of semi-submersible when it alone to interaction condition by experimental approach [14]. Besides that, K.U. Tiau (2012) was simulating the motion of mobile floating harbour which has similar hull form as semi-submersible by using Morison Equation [15]. In addition, C. L. Siow et.al also examined the heave damping efficiency for semi-submersible calculated by the diffraction potential theory at the damping dominate region and then they also propose an viscous damping correction method to increase the heave damping to improve the numerical result [19].

## 3.0 MATHEMATICAL MODEL

### 3.1 Diffraction Potential

In this study, the diffraction potential method was used to obtain the wave force act on the semi-submersible structure also the added mass and damping for all six directions of motions. The regular wave acting on floating bodies can be described by

velocity potential. The velocity potential normally written in respective to the flow direction and time as below:

$$\Phi(x, y, z) = Re[\phi(x, y, z)e^{i\omega t}] \quad (1)$$

$$\phi(x, y, z) = \frac{g\zeta_a}{i\omega} \{\phi_0(x, y, z) + \phi_7(x, y, z)\} + \sum_{j=1}^6 i\omega X_j \phi_j(x, y, z) \quad (2)$$

where;  $g$  is gravity acceleration,  $\zeta_a$  is incident wave amplitude,  $X_j$  is motions amplitude,  $\phi_0$  is incident wave potential,  $\phi_7$  is scattering wave potential,  $\phi_j$  is radiation wave potential due to motions and  $j$  is direction of motion.

From the above equation, it is shown that total wave potential in the system is contributed by the potential of the incident wave, scattering wave and radiation wave. In addition, the phase and amplitude for both the incident wave and scattering wave is assumed to be the same. However, radiation wave potentials are affected by each type of motions of each single floating body inside system, where the total potential for radiation wave for the single body is the summation of the radiation wave generates by each type of body motions such as roll, pitch, yaw, surge, sway and heave.

Also, the wave potential  $\phi$  must be satisfied with boundary conditions as below:

$$\nabla^2 \phi = 0 \quad \text{for } 0 \leq z \leq h \quad (3)$$

$$\frac{\partial \phi}{\partial z} + k\phi \quad \text{at } z = 0 \quad (k = \frac{\omega^2}{g}) \quad (4)$$

$$\frac{\partial \phi}{\partial z} = 0 \quad \text{at } z = h \quad (5)$$

$$\phi \sim \frac{1}{\sqrt{r}} e^{-ik_0 r} \quad \text{should be 0 if } r \rightarrow \infty \quad (6)$$

$$\frac{\partial \phi}{\partial n} = -\frac{\partial \phi_0}{\partial n} \quad \text{on the body boundary} \quad (7)$$

### 3.2 Wave Potential

By considering the wave potential only affected by structure surface,  $S_H$ , the wave potential at any point can be presented by the following equation:

$$\phi(P) = \iint_{S_H} \left\{ \frac{\partial \phi(Q)}{\partial n_Q} G(P; Q) - \phi(Q) \frac{\partial G(P; Q)}{\partial n_Q} \right\} dS(Q) \quad (8)$$

where  $P = (x, y, z)$  represents fluid flow pointed at any coordinate and  $Q = (\xi, \eta, \zeta)$  represent any coordinate,  $(x, y, z)$  on structure surface,  $S_H$ . The green function can be applied here to estimate the strength of the wave flow potential. The green function in eq. (8) can be summarized as follow:

$$G(P; Q) = -\frac{1}{4\pi\sqrt{(x-\xi)^2 + (y-\eta)^2 + (z-\zeta)^2} + H(x-\xi, y-\eta, z+\zeta)} \quad (9)$$

where  $H(x-\xi, y-\eta, z+\zeta)$  in eq. (9) represent the effect of free surface and can be solved by second kind of Bessel function.

### 3.3 Wave Force, Added Mass and Damping

The wave force or moment act on the structure to cause the motions of structure can be obtained by integral the diffraction wave potential along the structure surface.

$$E_i = -\iint_{S_H} \phi_D(x, y, z) n_i dS \quad (10)$$

where,  $\phi_D$  is diffraction potential,  $\phi_D = \phi_0 + \phi_7$

The added mass,  $A_{ij}$  and damping,  $B_{ij}$  for each motion can be obtained by integral the radiation wave due to each motion along the structure surface.

$$A_{ij} = -\rho \iint_{S_H} Re[\phi_j(x, y, z)] n_i dS \quad (11)$$

$$B_{ij} = -\rho\omega \iint_{S_H} Im[\phi_j(x, y, z)] n_i dS \quad (12)$$

$n_i$  in eq. (10) to eq. (12) is the normal vector for each direction of motion,  $i = 1 \sim 6$  represent the direction of motion and  $j = 1 \sim 6$  represent the six type of motions.

### 3.4 Drag Term of Morison Equation

The linear drag term due to the wave effect on floating structure is calculated using Drag force equation as given by Morison equation:

$$F_D = \frac{1}{2} \rho A_{proj} C_D |\dot{\phi}_Z - \dot{X}_Z| (\dot{\phi}_Z - \dot{X}_Z) \quad (14)$$

where  $\rho$  is fluid density,  $A_{proj}$  is projected area in Z direction,  $C_D$  is drag coefficient in wave particular motion direction,  $\dot{\phi}_Z$  is velocity of particle motion at Z-direction in complex form and  $\dot{X}_Z$  is structure velocity at Z-direction

In order to simplify the calculation, the calculation is carried out based on the absolute velocity approach. The structure dominates term is ignored in the calculation because it is assumed that the fluid particular velocity is much higher compared to structure velocity. Expansion of the equation (14) is shown as follows:

$$F_D = \frac{1}{2} \rho A_{proj} C_D |\dot{\phi}_Z| (\dot{\phi}_Z) - \frac{1}{2} \rho A_{proj} C_D |\dot{\phi}_Z| \dot{X}_Z - \frac{1}{2} \rho A_{proj} C_D |\dot{X}_Z| \dot{\phi}_Z + \frac{1}{2} \rho A_{proj} C_D |\dot{X}_Z| \dot{X}_Z \quad (15)$$

By ignoring all the term consist of  $|\dot{X}_Z|$ , equation (15) can be reduced into following format.

$$F_D = \frac{1}{2} \rho A_{proj} C_D |\dot{\phi}_Z| (\dot{\phi}_Z) - \frac{1}{2} \rho A_{proj} C_D |\dot{\phi}_Z| \dot{X}_Z \quad (16)$$

The above equation (16) is still highly nonlinear and this is impossible to combine with the linear analysis based on diffraction potential theory. To able the drag force to join with the diffraction force calculated with diffraction potential theory, the nonlinear drag term is then expanded in Fourier series. By using the Fourier series linearization method, equation (16) can be written in the linear form as follow:

$$F_D = \frac{1}{2}\rho A_{Proj} C_D \frac{8}{3\pi} V_{max} (\dot{\phi}_z) - \frac{1}{2}\rho A_{Proj} C_D \frac{8}{3\pi} V_{max} \ddot{X}_z \quad (17)$$

where,  $V_{max}$  in equation (17) is the magnitude of complex fluid particle velocity in Z direction. From the equation (17), it can summarize that the first term is linearize drag force due to wave and the second term is the viscous damping force due to the drag effect.

According to Christina Sjöbris, the linearize term  $\frac{8}{3\pi} V_{max}$  in the equation (17) is the standard result which can be obtained if the work of floating structure performance at resonance is assumed equal between nonlinear and linearized damping term [21].

The linearized drag equation as shown in equation (17) now can be combined with the diffraction term which calculated by diffraction potential theory. The modified motion equation is shown as follows:

$$(m + m_a)\ddot{X}_z + \left(b_p + \frac{1}{2}\rho A_{Proj} C_D \frac{8}{3\pi} V_{max}\right)\dot{X}_z + kx = F_p + \frac{1}{2}\rho A_{Proj} C_D \frac{8}{3\pi} V_{max} (\dot{\phi}_z) \quad (18)$$

where  $m$  is mass,  $k$  is restoring force,  $m_a$ ,  $b_p$ ,  $F_p$  is heave added mass, heave diffraction damping coefficient and heave diffraction force calculated from diffraction potential method respectively.  $\frac{1}{2}\rho A_{Proj} C_D \frac{8}{3\pi} V_{max}$  is the viscous damping and  $\frac{1}{2}\rho A_{Proj} C_D \frac{8}{3\pi} V_{max} (\dot{\phi}_z)$  is the drag force based on drag term of Morison equation.

### 3.5 Differentiation of Wave Potential for Morison Drag Force

To obtain the drag force contributed to heave motion, the wave particle velocity at heave direction must be obtained first. This water particle motion is proposed to obtain from the linear wave potential equation. From the theoretical, differential of the wave potential motion in Z-direction will give the water particle motion in the Z-direction.

As mentioned, the drag force in Morison equation is in the function of time; therefore, the time and space dependent wave potential in the complex should be used here. The wave potential in Euler form as follows:

$$\phi(x, y, z) = \frac{sg}{w} e^{-Kz+iKR+i\alpha} \quad (19)$$

The expanding for the equation (19) obtained that

$$\phi(x, y, z) = \frac{sg}{w} e^{-Kz} \cdot [\cos(KR) + i \sin(KR)] \cdot [\cos \alpha + i \sin \alpha] \quad (20)$$

Rearrange the equation (20), the simplify equation as follows

$$\phi(x, y, z) = \frac{sg}{w} e^{-Kz} \cdot [\cos(KR + \alpha) + i \sin(KR + \alpha)] \quad (21)$$

Differentiate the equation (21) to the Z-direction, the water particle velocity at Z-direction is shown as follows:

$$\phi_z(x, y, z) = \frac{sg}{w} (-K) e^{-Kz} \cdot [\cos(KR + \alpha) + i \sin(KR + \alpha)] \quad (22)$$

Since this numerical model is built for deep water condition, hence it can replace the equation by  $Kg = w^2$  and the equation (22) is becoming as follow:

$$\phi_z(x, y, z) = \zeta w e^{-Kz} \cdot [\cos(KR + \alpha) + i \sin(KR + \alpha)] \quad (23)$$

In the equations (19) to (23),  $\zeta$  is the wave amplitude,  $g$  is the gravity acceleration,  $w$  is the wave speed,  $K$  is wave number,  $R$  is the horizontal distance referring to zero coordinate,  $\alpha$  is the time dependent variable.

The horizontal distance,  $R$  and the time dependent variable,  $\alpha$  can be calculated by the following equation

$$R = Kx \cos \beta + Ky \sin \beta \quad (24)$$

$$\alpha = wt + \epsilon \quad (25)$$

In equation (24) and equation (25), the variable  $\beta$  is wave heading angle,  $\epsilon$  is the leading phase of the wave particle velocity at the Z-direction and  $t$  is time.

To calculate the drag forces by using the Morison equation, equation (23) can be modified by following the three assumptions below.

First, since the Morison equation is a two dimensional method, therefore the projected area of the Z-direction is all projected at the bottom of the semi-submersible.

Second, as mentioned in the previous part, this method applies the absolute velocity method and the heave motion of semi-submersible is considered very small and can be neglected; therefore, the change of displacement in Z-direction is neglected.

Third, by applying the concept of oscillation motion; we can obtain that the maximum speed will occur at minimum displacement. Hence, the maximum speed and the maximum displacement are always different by the angle  $\pi/2$ .

From the first and second assumption, the variable  $z$  at equation (23) is no effected by time and it is a constant and equal to the draught of the structure. Also, using the third assumption, it can be assumed that the leading phase  $\epsilon$  for the water particle velocity at Z-direction is always a constant and have the value of  $\pi/2$ .

Finally, by apply the trigonometry function where  $\cos(C + \pi/2) = -\sin(C)$  and  $\sin(C + \pi/2) = \cos(C)$ , then the equation (23) can be become as follow:

$$\phi_z(x, y, z) = \zeta w e^{-Kz} \cdot [-\sin(KR + wt) + i \cos(KR + \alpha)] \quad (26)$$

### 3.6 Determination of Drag Coefficient

Typically the drag coefficient can be identified from experimental results for the more accurate study. In this study, the drag coefficient is determined based on previous empirical data. To able the previous empirical used in this study, the pontoon for this semi-submersible is assumed as a horizontal cylinder. By referring to the most of the Fluid Mechanic book, it is obtained that the drag coefficient,  $C_D$  for the cylinder with different aspect ratio,  $\frac{Length, L}{Diameter, D}$  as shown in figure 1 in laminar flow condition is given as in table 1.

X

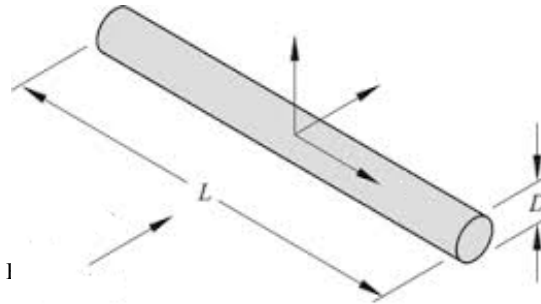


Figure 1: Horizontal Cylinder and flow direction.

Table 1: Drag Coefficient for Horizontal Cylinder [16]:

Aspect Ratio, $AR^{Length, L / Diameter, D}$	Drag Coefficient, $C_D$
$1 \leq$	0.6
2	0.7
5	0.8
10	0.9
40	1.0
$40 >$	1.2

The sample of pontoon for this semi-submersible is shown as follow.

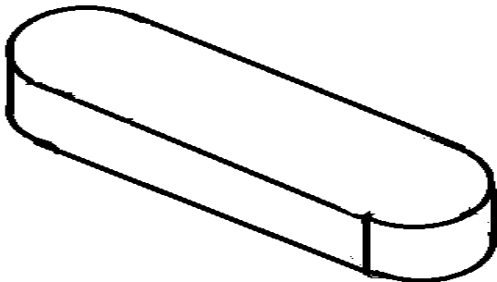


Figure 2: Isometric view for semi-submersible pontoon.

To obtain the aspect ratio for this pontoon, an imaginary radius for the non-round shape pontoon should be obtained as shown in figure 3.

As shown in figure 3, the imaginary radius for the semi-submersible cross section can be calculated by following equation of the depth and breadth for the pontoon is known.

$$R = \sqrt{\left(\frac{d}{2}\right)^2 + \left(\frac{b}{2}\right)^2} \quad (27)$$

Finally, the aspect ratio for the pontoon of semi-submersible for the flow acting in Z-direction can be obtained from the following equation

$$AR = \frac{L}{2R} \quad (28)$$

where L is the overall pontoon length and R is pontoon imaginary cross section radius calculate by equation (24)

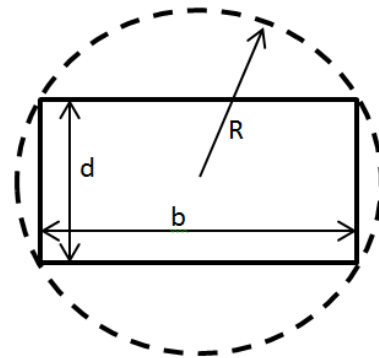


Figure 3: Front view for semi-submersible pontoon where R= Imaginary radius, d = Pontoon Depth, b = pontoon Breadth.

#### 4.0 MODEL PARTICULAR

As mentioned, the semi-submersible model was selected as the test model in this study. This Semi-submersible model was constructed based on GVA 4000. The model has four circular columns connected to two pontoons and two braces. Two pieces of plywood are fastened to the top of the Semi-submersible to act as two decks to mount the test instruments. The model was constructed from wood following the scale of 1:70 (Table 2).

Upon the model complete constructed, few tests were carried out to obtain the model particulars. Inclining test, swing frame test, oscillating test, decay test and bifilar test were carried out to identify the hydrostatic particular for the semi-submersible. The dimension and measured data for the model was summarized as in table 2.

Table 2: Principal particular of the Structures

Length	0.954 m
Width	0.835 m
Draft	0.239 m
Displacement	0.043501 m <sup>3</sup>
Water Plan Area	0.108082 m <sup>2</sup>
Number of Columns	4
Pontoon length	0.954 m
Pontoon depth	0.09 m
Pontoon width	0.19 m
Pontoons centerline separation	0.645 m
Columns longitudinal spacing (centre)	0.651143 m
Column diameter	0.151286 m
$GM_T$	0.041 m
$GM_L$	0.058 m
$K_{XX}$	0.452 m
$K_{YY}$	0.385 m
$K_{ZZ}$	0.5 m

#### 5.0 NUMERICAL SOLUTION SETUP

In this study, the numerical method applies to execute the motion response of semi-submersible will only estimate the wave force acting on the surface of the port side structure of semi-



submersible. After that, the total wave force for the semi-submersible is double before it fixed into the motion equation. The selected semi-submersible model in this study is constructed based on GVA 4000 type. Total panels used in the execution are 272 where 25 panels on each column and 222 panels on pontoon surface. The sample of mesh constructed by this numerical method for this semi-submersible model is shown in fig.4.

As similar with other diffraction potential method, this numerical method starts with mesh generation and then execute the normal vector, centre point of each panel and area for each panel. After that, the program will construct matrix element for distribution of sources and normal dipoles over the panel.

Next, wave force on each panel will executed by using green function and Bessel function. At this moment, radiation force and diffraction will be considered. After that, the total wave force acting on the structure to cause the motion can be obtained by summing up the total diffraction force on each panel. At the same time, added mass and damping of the structure at same wave condition can be obtained by summing up the real part of radiation potential and imaginary part of radiation potential.

If the drag term correction for heave motion is required, then the drag force and viscous damping for this motion will be executed based on the method explained in part 3.3. The required information used for the drag force calculation such as the structure offset, hydrostatic particular, wave data are same with the diffraction potential method. Calculated drag force and viscous damping are then stored in extra matrix independently before it is added to the motion equation follow the vector summation method. Lastly, the structure motion and its response to the wave can be obtained by solving the coupled motion equation.

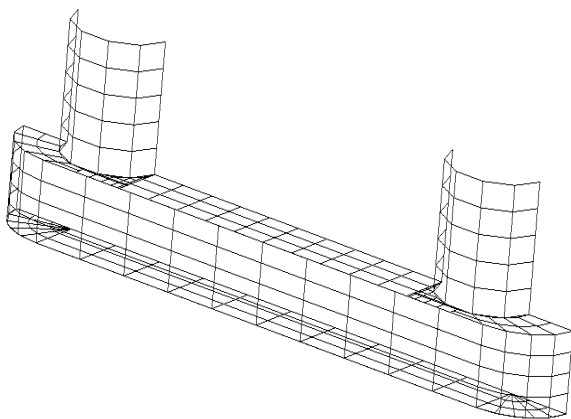


Figure 4: meshing for semi-submersible model.

## 6.0 RESULTS AND DISCUSSION

The previous study obtained that the diffraction potential theory is weak in predicting the heave motion response when the wave frequency close to the structure natural frequency [18]. By detail study of the problem, it is obtained that the linear damping predicted by the diffraction potential theory is very small at the wave condition and this caused the theory to give the infinite response at the wave condition [19].

Besides, the wave force at the wave frequency around the structure natural frequency predicted by the diffraction theory also obtained small and lead to the wrong prediction of heave response if compared to experiment result. In the diffraction potential theory, the force acting on the structure is obtained by integrating the pressure distributes of the structure surface and the force is acting in the direction of the surface normal vector. The surface will contribute to the heave motion for semi-submersible structure is located at the top side of the pontoon and the bottom side of the pontoon. When the wave frequency near to the structure natural frequency, it is obtained that the wave force acting on the top side of the pontoon is nearly same to the wave force acting on the bottom side of the pontoon. This phenomenon caused the cancellation of heave force and then leads to small response predicted on this wave condition.

### 6.1 Heave Damping

In this part, the discussion on heave motion response will focus on the effect of extra drag term to the motion equation and the calculated heave response amplitude operator. The damping coefficient and the heave force calculated by both the method will be first presented before the heave motion response calculated by this proposed method.

The figure 5 shown the non-dimensional heave damping calculated by diffraction potential theory, Morison drags term and summation of both the heave damping by both the method. From the comparison, it is obtained that the heave damping calculated by both the method is same for wavelength under 1.5 meters. After wavelength equal to 1.5 meters, it is obtained that the damping coefficient calculated by the diffraction potential theory decrease significantly and reduced to nearly zero after wave length 5 meters. From the study, the region where the heave motion dominates by damping term is at the location where the wave frequency is close to the structure natural frequency [22]. Due to the small prediction of the heave damping by diffraction potential theory, the motion response calculated in this region is becomes significantly large and no agreed to the experiment result.

On the other hand, the heave viscous damping calculated by the Morison drags term is keep increasing for wavelength longer than 1.5 meters. The heave damping predicted by the Morison drag term is predicted will become a constant if the wavelength becomes significant long as presented in figure 5. The opposite of the damping tendency between both the theories can be helped to correct the total damping value calculated from different methods.

To obtain the total damping for semi-submersible heave motion, the magnitude of damping coefficient is assumed can be directly sum up for the damping calculated by both the methods. As shown in figure 5, the total damping by sum-up the damping between the two methods will be influenced by the damping coefficient calculated by two of the methods for the wavelength below 5 meters. However, due to the damping calculated by diffraction potential theory for this semi-submersible is trending to become zero for wavelength longer than 5 meters, then the tendency of total damping will be followed the tendency of the viscous damping calculated by the Morison drag term. At understood, the heave motion dominated by damping term is falling in the structure natural frequency region. For this selected structure, it is obtained that the natural frequency of heave motion is located at a wavelength around 9 meters. By referring to the

figure 5, the damping coefficient obtained by summing up the damping calculated from both the methods given the magnitude around 1.2. At this calculated magnitude, it can summarize that the addition viscous damping by using Morison drags term can be helped to correct the damping coefficient and corrected the motion response estimated at the damping dominated region.

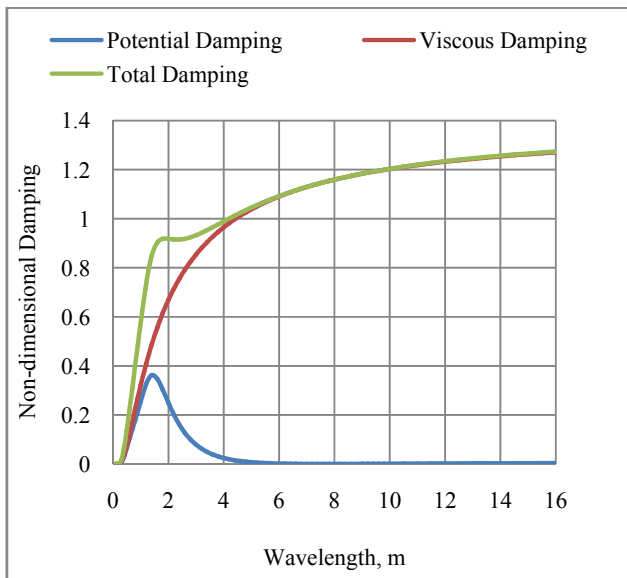


Figure 5: No dimensional Heave Damping for semi-submersible model

### 6.2 Morison Drag Force and Heave Force

Besides smaller predicted heave damping, the heave force also under-predicted by diffraction potential theory. As mentioned in the earlier, the small predicted heave force is due to the cancellation of force due to the pressure distribution on the top side and bottom side of the pontoon. As shown in figure 6, the heave force predicted by the diffraction potential theory experience this force cancellation phenomenon at the wavelength around 7.5 meters. At this wavelength, it is obtained that the heave motion response calculated by this diffraction potential theory is dropped to nearly zero and give a non-rational result.

As shown in figure 6, the heave force calculated by the diffraction potential theory will increase significantly from wavelength 0 meter to wave length 1.6 meters and then follow by significant reductions by increasing of wavelength until where the calculated wave force become nearly zero at a wavelength around 7.5 meters for this selected semi-submersible structure. After the significant drop, the heave force calculated by this diffraction potential theory will increase gradually when wavelength increasing.

For the drag force calculated by Morison drag term, it is obtained that the tendency of heave force is different compared to the heave force calculated by the diffraction potential theory. The heave force calculated by the Morison drag term is increasing rapidly from wavelength 0.5 meters to wave length 3.4 meters before it is reduced slowly to zero drag heave force by increase of wavelength.

To combine the heave force contributed by both the methods, the summation of force is similar to the method of combining the initial force and drag force applied in Morison equation. In this study, the heave force calculated by the diffraction potential theory is assumed as the initial force term in the Morison equation. At the same time, the drag term for the total force is contributed by the linearly drag force from the drag term of the Morison equation. Both the heave force contributed by both the method is total up by vector summation theory.

By referring to figure 6, it is obtained that the tendency of total heave force which total up by involved the diffraction force and drag force will no return to zero compared to the heave force calculated by diffraction potential methods. From the figure, it is observed that the total heave force will follow the diffraction force for the region of wave length other than 7.5 meters due to the diffraction force is significantly higher compared to the drag force. The role of the drag force in this calculation is to correct the heave force in the region where cancellation of force occurred in the diffraction potential theory. By the existing of the drag force from the Morison drag term, it is obtained that the drag force is shifted to the acceptable level and did not trend down to become zero where it is the main factor to causing the absolutely low heave motion response made by diffraction theory at the region.

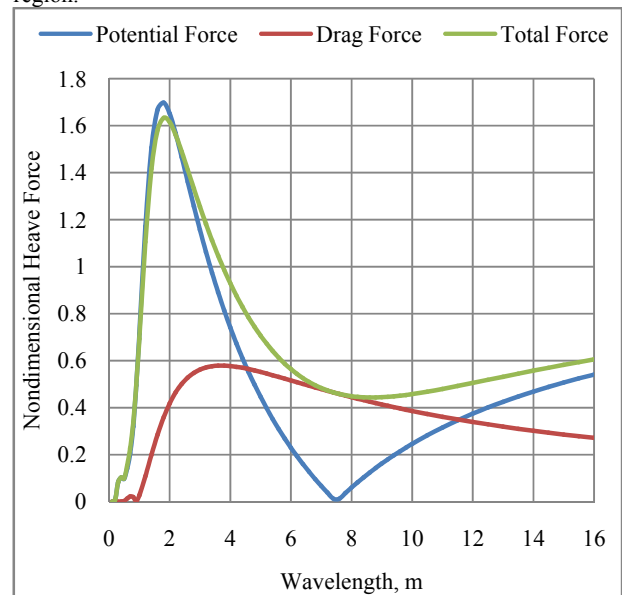


Figure 6: Heave force semi-submersible model

### 6.3 Heave Motion Response

The heave RAO calculated by the diffraction potential theory and the corrected diffraction potential theory by the Morison drag term is presented in figure 7. The experimental data collected is only ranged from wavelength around 1 meter to wavelength around 9 meters due to the limitation of the wave generating device in the laboratory. Comparison between the heave response calculated by the diffraction potential theory with and without Morison drag term correction is also presented in the figure 7. From the figure, it can be obtained that the diffraction potential theory with drag term correction is more accurate compared to the one without correction. The tendency of the heave response

calculated by the diffraction potential theory with and without drag correction method shown non-similarity start from the wavelength around 3 meters. The calculated numerical result without the Morison drag correction is no agree with to the experimental result especially in the region where the wave frequency closed to the structure natural frequency (wave length equal to 9 meters). It can be observed that the drag force from the Morison equation is significantly important to estimate the heave motion response for semi-submersible structure in figure 7. By involving the drag effect for the calculation, the tendency of the numerical result will closer to the experimental result. Therefore, it can be summarized the neglected of the drag effect on the estimate heave response of semi-submersible like the diffraction potential theory will lead to wrong prediction of heave response in the region where the motion is dominated by damping. The reason for this observation are also explained in the figure 5 and 6 where it can obtain that the damping coefficient and heave force is under-predicted by the diffraction potential theory.

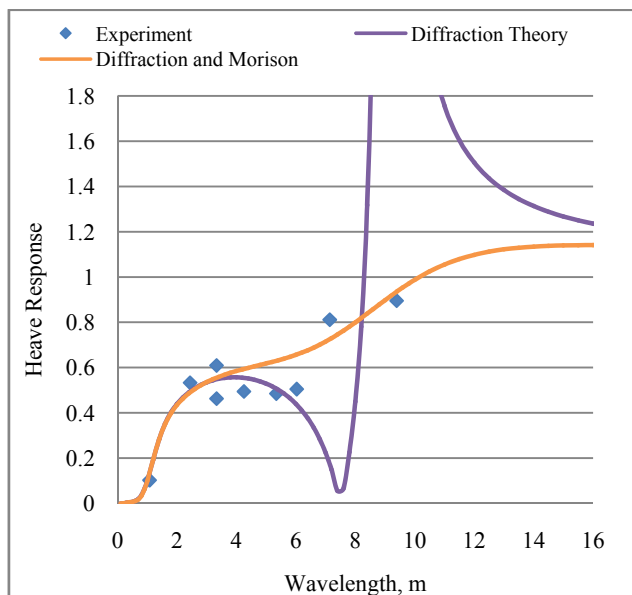


Figure 7: Heave motion responses for semi-submersible model

## 6.0 CONCLUSION

In the conclusion, this paper was presented the correction method to improve the tendency of heave response calculated by the diffraction potential theory. In general, the diffraction potential theory is a good method to predict the motion of offshore structure especially semi-submersible in short time. Compare to the experimental result, it is obtained that the pure diffraction potential theory will wrong predicted the heave response in the region where the heave motion is dominated by damping or drag term. The weakness of the diffraction potential theory to neglect the drag effect was caused the damping and the heave force smaller than the actual situation and lead to wrong heave response tendency at the damping and drag dominate region. By involving the drag calculation using the drag term from Morison equation, the less accurate of damping and heave force calculated by

diffraction potential theory can be corrected. In this paper, the numerical results calculated by the proposed method shown that the surge, pitch and heave motion response in head sea condition are agreed between the numerical result and experiment result. Therefore, it can be concluded that the diffraction potential theory with the Morison drag correction can be a suitable numerical approach to estimate the motion of offshore floating structure especially semi-submersible structured.

## ACKNOWLEDGEMENTS

The authors would like to gratefully acknowledge to Marine Technology Center, Universiti Teknologi Malaysia for supporting this research.

## REFERENCE

- Hess, J. L., Smith, A. M. O., (1964). *Calculation of Nonlifting Potential Flow About Arbitrary 3D Bodies*, Journal of Ship Research.
- Van Oortmerssen, G., (1979). Hydrodynamic interaction between two structures of floating in waves, *Proc. of BOSS '79. Second International Conference on Behavior of Offshore Structures*, London.
- Loken, E., (1981). Hydrodynamic interaction between several floating bodies of arbitrary form in Waves, *Proc. of International Symposium on Hydrodynamics in Ocean Engineering*, NIT, Trondheim.
- Wu, S., Murray, J. J., Virk, G. S., (1997). *The motions and internal forces of a moored semi-submersible in regular waves*, Ocean Engineering, 24(7), 593-603.
- Yilmaz, A. Incecik, (1996). *Extreme motion response analysis of moored semi-submersibles*, Ocean Engineering, 23(6) 497-517.
- Söylemez, M., (1995). *Motion tests of a twin-hulled semi-submersible*, Ocean Engineering, 22(6) 643-660.
- Clauss, G. F., Schmittner, C., Stutz, K., (2002). Time-Domain Investigation of a Semi Submersible in Rogue Waves, *Proc. of the 21st International Conference on Offshore Mechanics and Arctic Engineering*, Oslo, Norway.
- Matos, V. L. F., Simos, A. N., Sphaier, S. H., (2011). *Second-order resonant heave, roll and pitch motions of a deep-draft semi-submersible: Theoretical and Experimental Results*, Ocean Engineering, 38(17-18) 2227-2243.
- Wackers, J. et al., (2011). *Free-Surface Viscous Flow Solution Methods for Ship Hydrodynamics*, Archive of Computational Methods in Engineering, Vol. 18 1-41.
- Afrizal, E., Mufti, F.M., Siow, C.L., Jaswar, (2013). Study of Fluid Flow Characteristic around Rounded-Shape FPSO Using RANS Method, *The 8th International Conference on Numerical Analysis in Engineering*, pp: 46 - 56, Pekanbaru, Indonesia.
- Jaswar et al, (2011). An integrated CFD simulation tool in naval architecture and offshore (NAO) engineering, *The 4th International Meeting of Advances in Thermofluids, Melaka, Malaysia, AIP Conf. Proc.* 1440, pp: 1175-1181.
- Abyn, H., Maimun, A., Jaswar, Islam, M. R., Magee, Bodagi, A., B., Pauzi, M., (2012). Model Test of Hydrodynamic Interactions of Floating Structures in Regular Waves, *Proc. of*



- the 6<sup>th</sup>Asia-Pacific Workshop on Marine Hydrodynamics*, pp: 73 - 78, Malaysia.
13. Abyn, H., Maimun, A., Jaswar, Islam, M. R., Magee, A., Bodagi, B., Pauzi, M., (2012). Effect of Mesh Number on Accuracy of Semi-Submersible Motion Prediction, *Proc. of the 6<sup>th</sup>Asia-Pacific Workshop on Marine Hydrodynamics*, pp: 582 - 587, Malaysia.
  14. Siow, C. L., Jaswar, Afrizal, E., Abyn, H., Maimun, A., Pauzi, M., (2013). Comparative of Hydrodynamic Effect between Double Bodies to Single Body in Tank, *The 8<sup>th</sup>International Conference on Numerical Analysis in Engineering*, pp: 64 – 73, Pekanbaru, Indonesia.
  15. Tiau, K.U., Jaswar, Hassan Abyn and Siow, C.L., (2012). Study On Mobile Floating Harbor Concept, *Proc. of the 6<sup>th</sup>Asia-Pacific Workshop on Marine Hydrodynamics*, pp: 224 - 228, Malaysia.
  16. Cengel, Y. A., Cimbala, J. M. (2010). *Fluid Mechanics Fundamentals and Application*. 2<sup>nd</sup> Ed.
  17. Kvittem, M. I., Bachynski, E.E., Moan, T., (2012). Effect of Hydrodynamic Modeling in Fully Coupled Simulations of a Semi-Submersible Wind Turbine, *Energy Procedia*, 24.
  18. Siow, C. L., Abby Hassan, and Jaswar, (2013). Semi-Submersible's Response Prediction by Diffraction Potential Method, *The International Conference on Marine Safety and Environment*, pp: 21 - 28, Johor, Malaysia.
  19. Siow, C. L., Jaswar, K., and Abby Hassan, (2014). Semi-Submersible Heave Response Study Using Diffraction Potential Theory with Viscous Damping Correction. *Journal of Ocean, Mechanical and Aerospace Science and Engineering*, Vol. 5.
  20. Nallayarasu, S. and Siva Prasad, P., (2012). Hydrodynamic Response of Spar and Semi-submersible Interlinked by a Rigid Yoke - Part 1: *Regular Wave, Ship and Offshore Structures*, 7(3).
  21. Christina Sjöbris, (2012). Decommissioning of SPM buoy, *Master of Science Thesis*, Chalmers University of Technology, Gothenburg, Sweden.
  22. Journee, J.M.J and Massie, W.W. (2001). *Offshore Hydromechanics. (1<sup>st</sup> Edition.)*, Delf University of Technology.